



**LEVEL**

(12)

NRL Memorandum Report 204

# Application of Ferrofluids as an Acoustic Transducer Material

PIETER S. DUBBELDAY

*Transducer Branch  
Underwater Sound Reference Detachment  
P.O. Box 8337, Orlando, FL 32856*

ADA 079314

December 4, 1979



D D C  
RECEIVED  
JAN 11 1980  
A

DDC FILE COPY

79 12 19 204

NAVAL RESEARCH LABORATORY  
Washington, D.C.

Approved for public release; distribution unlimited.

9 REPORT DOCUMENTATION PAGE		READ INSTRUCTIONS BEFORE COMPLETING FORM
1. REPORT NUMBER NRL Memorandum Report 030	2. GOVT ACCESSION NO.	3. RECIPIENT'S CATALOG NUMBER
6 APPLICATION OF FERROFLUIDS AS AN ACOUSTIC TRANSDUCER MATERIAL		5. TYPE OF REPORT & PERIOD COVERED Interim report on a continuing NRL problem.
7. AUTHOR 10 Pieter S. Dubbelday		6. PERFORMING ORG. REPORT NUMBER
9. PERFORMING ORGANIZATION NAME AND ADDRESS Naval Research Laboratory (Washington, DC 20375) Underwater Sound Reference Detachment P.O. Box 8337, Orlando, FL 32856		8. CONTRACT OR GRANT NUMBER(s) N00172-D-0007 Project Order 009
11. CONTROLLING OFFICE NAME AND ADDRESS		10. PROGRAM ELEMENT, PROJECT, TASK AREA & WORK UNIT NUMBERS NRL Problem S02-38.101 PE 61153N.17 17 Design RR0110842
14. MONITORING AGENCY NAME & ADDRESS (if different from Controlling Office) 12 30		11. DATE 4 December 1979
16. DISTRIBUTION STATEMENT (of this Report) Approved for public release; distribution unlimited.		13. NUMBER OF PAGES 29
17. DISTRIBUTION STATEMENT (of the abstract entered in Block 20, if different from Report) 14 NRL-MR-4030		15. SECURITY CLASS (of this report) UNCLASSIFIED
18 SBIE		15a. DECLASSIFICATION/DOWNGRADING SCHEDULE
19 AD-E 000 343		
16 RR01108		
16. SUPPLEMENTARY NOTES *Oak Harbour Marine Associates, Inc., P. O. Box 8481, Southport, Florida 32409		
19. KEY WORDS (Continue on reverse side if necessary and identify by block number) Ferrofluids Electroacoustic transducers Transducer material		
20. ABSTRACT (Continue on reverse side if necessary and identify by block number) Application of ferrofluids to electroacoustic transduction is described. Properties of ferrofluids relevant to the problem are given, and the basic equations and derivations are developed. Power transfer calculations are performed for a piston-type transducer, and a conceptual design is offered for a toroidal configuration.		

251 950

gjk

7
ounced
ication
Codes
1/or
special

CONTENTS

INTRODUCTION. . . . . 1

General Properties of Ferrofluids . . . . . 1

Mode of Transduction. . . . . 2

Basic Equations . . . . . 2

DRIVING FORCE . . . . . 4

M(H) Curve for a Ferrofluid . . . . . 4

Operating Point . . . . . 7

APPLICATION TO PISTON TRANSDUCER. . . . . 8

Conceptual Design . . . . . 8

Power Transfer Calculations . . . . . 10

Optimization of Acoustic Power Output . . . . . 12

APPLICATION TO TOROIDAL TRANSDUCER. . . . . 13

CONCLUSIONS AND RECOMMENDATIONS . . . . . 16

REFERENCES. . . . . 17

APPENDIX A - Properties of Commercial Ferrofluids . . . . . 19

APPENDIX B - Sample Calculations of Acoustic Power. . . . . 22

## APPLICATION OF FERROFLUIDS AS AN ACOUSTIC TRANSDUCER MATERIAL

### INTRODUCTION

#### General Properties of Ferrofluids

Ferrofluids are composed of subdomain ( $\sim 10$  nm) ferromagnetic particles, colloidally suspended in a carrier fluid. The particles are prevented from flocculating by a surfactant, e.g., oleic acid. The carrier is typically nonconductive, but efforts are in progress to suspend the particles in conducting liquids such as mercury or gallium. Commercially available ferrofluids together with their properties are listed in Table A1 of Appendix A.

The nature of the ferrofluid points directly to a possible use in acoustical transduction. For this report, the properties of the material were studied from the viewpoint of this intended application. Two conceptual designs are presented for transducers, and power transfer is computed on the basis of typical values for the ferrofluid properties.

An exhaustive literature survey will not be offered, but reference is made to a limited number of key sources, from where further penetration into the literature will be simple. The most comprehensive source is the book edited by Berkovsky [1]. Other useful survey articles are those by Bashtovoi and Berkovskii [2], Berkovsky and Rosensweig [3] Bertrand [4], and Shliomis [5]. On the subject of acoustic transduction of ferrofluids, the literature is quite limited. A theoretical analysis is found in Cary and Fenlon [6]. Experimental work on electroacoustic transduction by ferrofluids is described in a thesis by Overby [7], and a patent concerning its feasibility has been applied for.

Note: Manuscript submitted July 6, 1979.

### Mode of Transduction

Cary and Fenlon [6] reach the conclusion that "at the present time it seems unlikely that ferrofluids can compete efficiently with conventional magnetostrictive materials for frequencies below 80 kHz, where these materials can be operated with tolerable efficiency." Even for higher frequencies they remain pessimistic with the conclusion: "Still, the magnetostrictive mode of operation does not provide a realistic engineering alternative at the present time." In contrast, they consider the piston mode of operation as a real alternative to existing transducer materials, especially above a frequency of 80 kHz. The reason for this frequency limitation is not quite clear. Admittedly, the piston mode of operation does not appear to utilize the fluid properties per se. Use of a soft iron cylinder would accomplish the same objective. In the latter case, hysteresis would be a disadvantage compared with the ferrofluid, but one could counteract this by distributing the particles of subdomain size in a solid matrix. For this report, the merits of the material in relatively low-frequency transduction were especially investigated. The first design, that of a cylindrical piston, is followed by a more tentative description of a toroidal configuration, whereby essential use is made of the fluid properties of the material.

### Basic Equations

Historically there has been considerable controversy concerning the proper formulation of the ponderomotive forces of the electromagnetic field. The issue is quite extensively, and presumably conclusively, dealt with in a monograph by Penfield and Haus [8]. Discussion of the controversy directly pertaining to ferrofluids together with simple examples are given by Jones [9]. An essential ingredient in the resolution of the apparent discrepancies between the various formulations is the realization that there is no experimental verification possible of the local stresses assumed in the theory. Any proposed measurement will amount to the introduction of a discontinuity in the

continuum. Thus, a certain arbitrariness in the differential formulation of the field-matter interaction is unavoidable; the result obtained by integration over a finite sample should be unambiguous, though. It follows that there is a certain freedom of choice between the various formulations, which is often decided by the particular application.

For the purpose of analysis of the piston mode of operation, to the exclusion of the magnetostrictive mode, the following set of equations appears useful, designated as the "Rosensweig-Neuringer ferrohydrodynamics equations for a nonconducting incompressible ferrofluid" by Berkovsky et al [10], and quoted from this source:

$$\frac{dT}{dt} = k\nabla^2 T \quad (1)$$

$$\frac{d\vec{v}}{dt} = -\frac{1}{\rho_0}\vec{\nabla}p + \nu\nabla^2\vec{v} + \frac{1}{\rho_0}\rho\vec{g} + \frac{\mu_0}{\rho_0}M\vec{\nabla}H \quad (2)$$

$$\text{div } \vec{v} = 0 \quad (3)$$

$$\text{curl } \vec{H} = 0 \quad \text{div } \vec{B} = 0 \quad \vec{M} = \frac{M}{H} \vec{H} \quad (4)$$

$$\rho_f = \rho_0(1 - \beta(T - T_0)) \quad M = M(T, H) \quad (5)$$

where  $\frac{d}{dt} = \frac{\partial}{\partial t} + (\vec{v} \cdot \vec{\nabla})\vec{v}$

T temperature

$\vec{v}$  velocity

$\vec{M}$  magnetization

$\vec{H}$  magnetic field strength

p pressure

$\rho_f$  density of ferrofluid

$\rho_0$  density of ferrofluid at reference temperature  $T_0$

- k thermal diffusivity
- $\nu$  kinematic viscosity
- $\mu_0$  magnetic permeability of vacuum
- $\beta$  thermal expansion coefficient
- g gravitational acceleration

It will be noticed that the equations consist of the Boussinesq approximation for the fluid motion augmented by a body force due to the interaction of magnetic field and magnetic moment. It is derived from the more general expression for the force per unit volume  $\mu_0 (\vec{M} \cdot \nabla) \vec{H}$ , by assuming that the magnetization  $\vec{M}$  is always in the direction of the magnetic field  $\vec{H}$ , and by the irrotationality of the magnetic field. The latter assumption implies that there are no true currents since the fluid is nonconducting, and that the displacement currents are negligible. The temperature equation and linearized equation of state are carried along for the sake of completeness, although they will not play a role in the present study. Limitation of the study to piston operation has as a consequence that the velocity is practically independent of position; and therefore the equation of motion reduces to the simpler form

$$\frac{\partial \vec{v}}{\partial t} = - \frac{1}{\rho_0} \nabla p + \frac{\mu_0}{\rho_0} \vec{M} \nabla H \quad (6)$$

#### DRIVING FORCE

##### M(H) Curve for a Ferrofluid

The functional relationship between magnetization and magnetic field in a ferrofluid can be adequately derived by the theory of superparamagnetism [11]. In this theory, it is assumed that "... single-domain ferromagnetic particles behave magnetically in a manner analogous to the Langevin paramagnetism of moment bearing atoms. The main distinction is that the moment of the particle may be  $10^5$  the atomic moment." Understanding some aspects of this theory will aid in judging

the intrinsic properties of the material and the range of operation in the M(H) diagram.

Investigation of the application of superparamagnetism to ferrofluids and its experimental aspects has been performed by Kaiser and Miskolczy [12]. Following their discussion, one can write the Langevin formula for the magnetization  $m_i$  of an isolated isotropic particle of volume  $v_i$  in an applied field H, as

$$\frac{m_i}{M_s} = \coth \frac{v_i M_s H}{4\pi kT} - \frac{4\pi kT}{v_i M_s H} \quad (7)$$

where k is Boltzmann's constant, T is the absolute temperature, and  $M_s$  is the domain magnetization.

The Langevin function (Fig. 1) shows the typical saturation behavior. Comparison with experimental values involves summation of the Langevin formula over particles of different sizes to arrive at an expression for  $M/(cM_s)$ , where M is the overall magnetization and c is the volumetric concentration of solids. The resulting curve gives a good fit to experiment only if one takes into account the presence of a non-magnetic surface layer due to the reaction of the surface atoms of magnetite with polar groups of the stabilizing agent used to prevent flocculation.

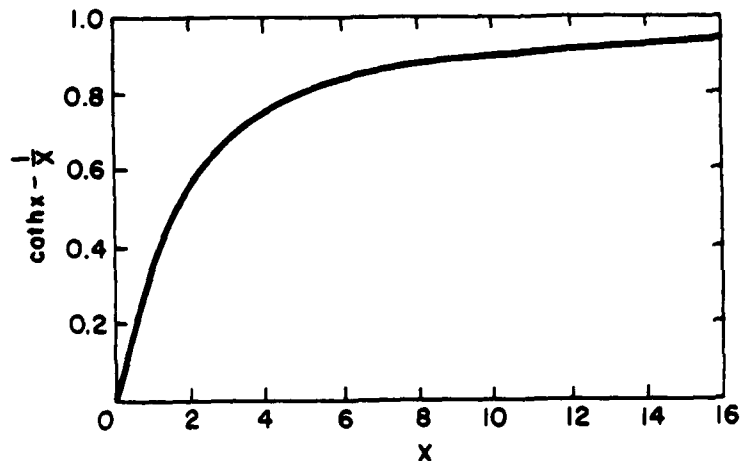


Fig. 1 - Graph of Langevin function

Figure 2 shows the resulting relative magnetization for the case of a hydrocarbon carrier, Figs. 3 and 4 for other carrier fluids.

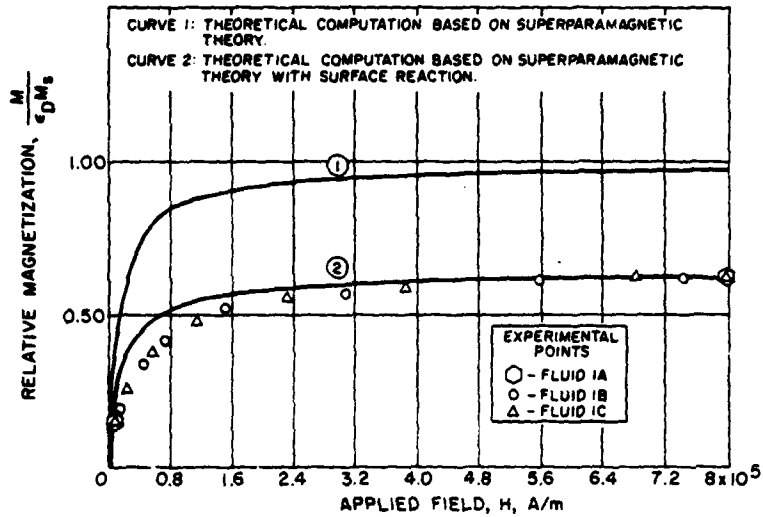


Fig. 2 - Magnetization curve for hydrocarbon base ferrofluids (From Kaiser and Miskolczy [12]). Copyright © 1970 by American Institute of Physics. Reprinted, by permission, from J. Appl. Phys. 41, 1064-1072 (1970).

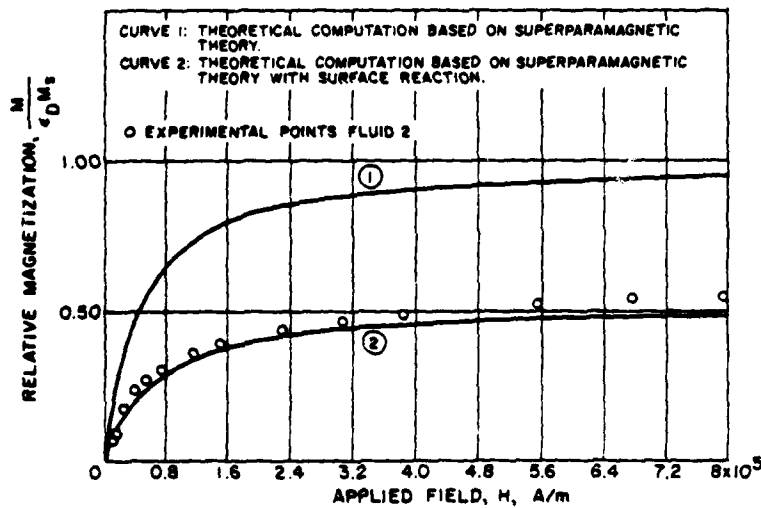


Fig. 3 - Magnetization curve for a fluorocarbon base ferrofluid (From Kaiser and Miskolczy [12]). Copyright © 1970 by American Institute of Physics. Reprinted, by permission, from J. Appl. Phys. 41, 1064-1072 (1970).

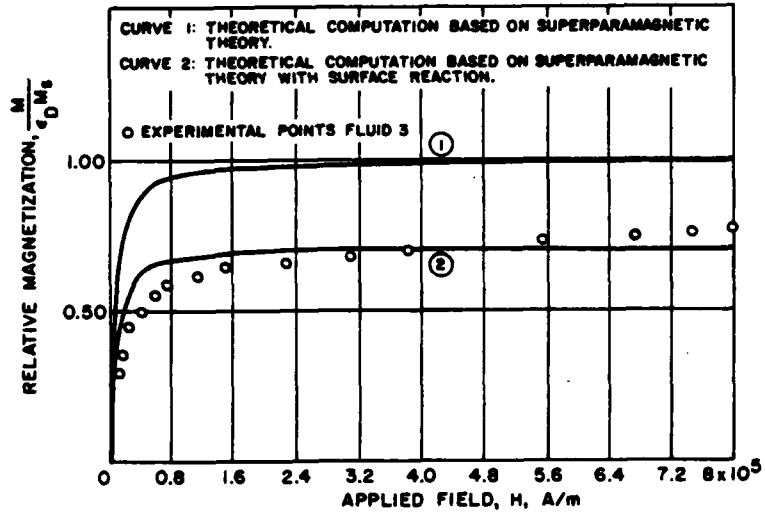


Fig. 4 — Magnetization curve for a waterbase ferrofluid (From Kaiser and Miskolczy [12]). Copyright © 1970 by American Institute of Physics. Reprinted, by permission, from J. Appl. Phys. 41, 1064-1072 (1970).

Kaiser and Miskolczy [12] do not offer an explanation for the fact that the waterbase fluid has a sharper transition to saturation than do the other fluids, while one would expect a behavior independent of the properties of the carrier. If the appearance of a sharper knee is an essential feature of a waterbase ferrofluid, it would indicate a considerable advantage, namely a lower operating point in a magnetic field and thus less dc power needed. The quantitative relationship for  $M$  can be derived since the saturation value for magnetite  $M_s = 5600 \text{ G}$  ( $4.5 \times 10^5 \text{ A/m}$ ); a 400-G ( $3.2 \times 10^4 \text{ A/m}$ ) fluid like kerosene H 01 B (Table A1) has a volumetric concentration,  $\epsilon$ , of 0.128.

#### Operating Point

There are essentially two possibilities for the operating point of a ferrofluid transducer. In the first place, one might operate at a zero bias field, with the advantage that no power is spent on creating a dc magnetic field. The obvious disadvantage is the fact that the force will be quadratic in terms of the ac current since both  $M$  and  $H$  would

be proportional to the current in the linear part of the  $M(H)$  curve, with the attending frequency doubling, harmonic distortion, and intermodulation. Moreover, the power produced for low amplitude becomes very small. Nevertheless, this operating point may be indicated for some applications.

It looks more attractive, though, to operate the ferrofluid at a point where there is virtual saturation such that the operation will be linear with the ac drive current. Since the differential susceptibility is practically zero, the calculation of the ac field will be less complicated. In the following discussion it is assumed that a dc field produces saturation and that an ac field is superimposed of such an amplitude that the total  $H$  field stays in the saturation region. An additional advantage is that one is not concerned about the various relaxation times of the demagnetization of the particles due to different mechanisms [13].

## APPLICATION TO PISTON TRANSDUCER

### Conceptual Design

Figure 5 shows a conceptual design for a ferrofluid transducer that forms the basis for the power-transfer calculations. The dc and ac fields are produced by separate solenoids because separation of the two components in a single coil offers more problems than the advantages would warrant and because of the field geometry. The ferrofluid is contained in a rigid cylindrical nonferromagnetic container, which is provided with a cone for improvement of coupling to the acoustic medium. The container slides inside the support pipe of the solenoids; friction is reduced by the use of dry lubricating material (e.g., Rulon J material, a product of Dixon Industries Corp., Bristol, RI). The container is kept in place by two springs with a small spring constant such that the resonance frequency will be well below the operating frequency.

The two faces of the ferrofluid container are located in the magnetic fields of two ac coils, with opposite sign. The two coils are

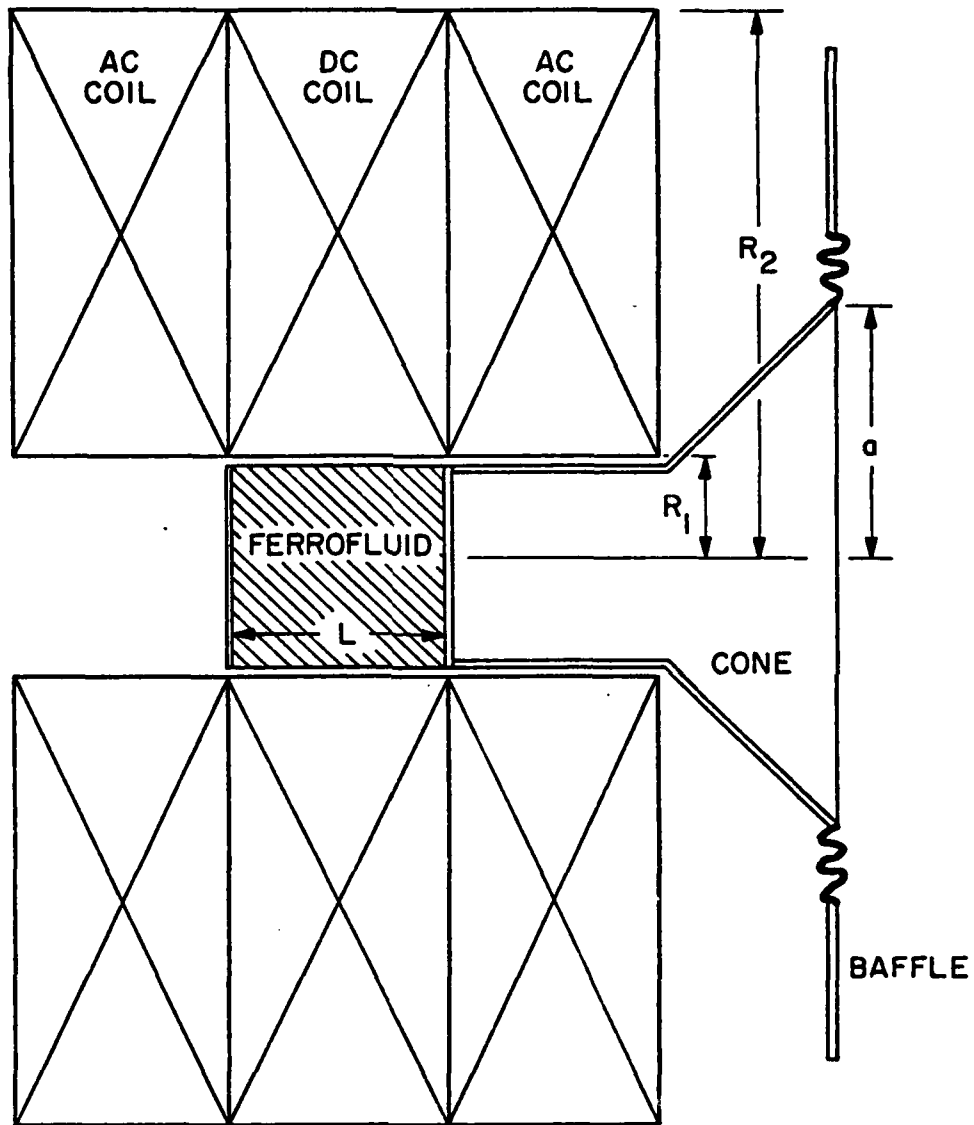


Fig. 5 - Conceptual design of piston-type transducer.

electrically in series but are wound in opposite directions. Apart from providing the opposite sign in the magnetic field, this arrangement results in a zero mutual inductance between dc and ac coils such that no ac potential is induced into the dc coil.

Design considerations for the coils will be discussed in a later section.

### Power Transfer Calculations

The transfer properties for an electroacoustic transducer are often represented as a two-port network by

$$E = Z_e I + T_{em} V \quad (8a)$$

$$F = T_{me} I + Z_m V \quad (8b)$$

where E the electric voltage

I the electric current

V the mechanical velocity

F the mechanical force

$T_{me} = T_{em}$ , the transfer coefficients, equal to each other in the linear region of operation.

The transfer coefficient  $T_{em}$  is derived from the total force exerted on the ferrofluid by the magnetic field

$$T_{me} I = \iiint \mu_0 M_0 \vec{V} H d(\text{vol}) \quad (9)$$

where  $M_0$  is the saturation magnetization.

By Gauss' theorem, this is equal to  $\mu_0 M_0 \iint \vec{H} dA$  where the integration is over the surface of the ferrofluid. In the case of a cylindrical transducer in an axially symmetric field, this becomes

$$\begin{aligned}
 T_{me} I &= \mu_o M_o \int_0^{R_1} \Delta H_z 2\pi r dr \\
 &= \mu_o M_o \overline{\Delta H_z} \pi R_1^2
 \end{aligned}
 \tag{10}$$

where  $\Delta H_z$  is the difference in magnetic field at corresponding points on the two cylinder faces and  $\overline{\Delta H_z}$  is the average of  $\Delta H_z$  over the cylinder faces.

The equation of motion (Eq. (6)) provides the relationship between the magnetic field and the displacement velocity  $V$  of the ferrofluid mass ( $M_f$ ) and the equation of motion with integration over the volume of the ferrofluid becomes

$$M_f \frac{\partial v}{\partial t} = - \int p dA + \mu_o M_o \overline{\Delta H_z} \pi R_1^2.
 \tag{11}$$

It is assumed that one of the cylinder faces is in practically pressure-free surroundings, so that the integral of the pressure is evaluated only over the cylinder face with the cone in contact with the acoustic medium.

According to the usual calculation of radiation loading of a circular piston [14] the relation of the pressure integral to the impedance is

$$2\pi \int_0^a p(r,0) dr = (R_p - i\omega M_p) V
 \tag{12}$$

where  $R_p$  is the radiation resistance and  $M_p$  is the accession to inertia. Thus, the magnetic force is given by

$$F_m = \mu_o M_o \overline{\Delta H_z} \pi R_1^2 = [R_p - i\omega(M_p + M_f) - \frac{K}{i\omega}] V
 \tag{13}$$

where  $K$  is the spring constant. It is assumed that the friction of the container is small compared with the radiation resistance. The average acoustic power output is given as

$$\Pi = \frac{1}{2} \text{Re}(F V^*) \quad (14)$$

where the asterisk indicates the complex conjugate, and thus

$$\Pi = \frac{1}{2} \left( \frac{F_m^2}{R_p} \right) \left( \frac{R_p^2}{R_p^2 + (M_f + M_p)^2 \omega^2} \right) \quad (15)$$

assuming that the frequency is well above resonance, which can be obtained by choosing the spring constant  $K$  small enough.

#### Optimization of Acoustic Power Output

Assessment of the various factors influencing the total acoustic power radiated by the ferrofluid transducer is facilitated by writing the power formula Eq. (15) in the following form, obtained by algebraic manipulation,

$$\Pi = \left[ \frac{\frac{1}{2} F_m^2}{(\rho c) (\pi R_1^2)} \right] \left[ \frac{R_1}{a} \right]^2 \left[ \frac{(\rho c) (\pi a^2)}{R_p} \right] \left[ \frac{\left\{ \frac{R_p}{(\rho c) (\pi a^2)} \right\}^2}{\left\{ \frac{R_p}{(\rho c) (\pi a^2)} \right\}^2 + (ka)^2 \left\{ \left( \frac{\rho_f}{\rho} \right) \left( \frac{R_1}{a} \right)^2 \left( \frac{L}{a} \right) + \frac{M_p}{\pi \rho a^3} \right\}^2} \right] \quad (16)$$

where  $\rho$  is the density of the medium.

The first factor,  $\frac{1}{2} F_m^2 / (\rho c) (\pi R_1^2)$ , can be interpreted as the power radiated by the cylindrical container, radius  $R_1$ , if the radiation resistance had the plane wave value  $\rho c$ . The factor  $(\rho c) (\pi a^2) / R_p$  corrects for this assumption and is the inverse of the dimensionless

expression for the radiation resistance as commonly graphed (Fig. B2) or tabulated (Table B1). The first three factors together represent the power radiated at resonance; the fourth factor corrects this to a frequency well away from resonance. The expression  $(M_p / \pi \rho a^3)$  is the usual form in graphs (Fig. B2) or tables (Table B1) for the dimensionless accession to mass.

No term is introduced for the mass of the cone in the overall power computation because it is difficult to give an analytical expression for this in terms of required stiffness and radius. Since the basic transducer material has high density, it is felt that this factor does not essentially alter the design optimum, although certainly its inclusion is necessary for "fine-tuning" the design.

The value of  $ka$  for the proposed design is not larger than 1, and thus the directivity of the transducer is negligible.

The tabulation of the various terms in Table B2 is not claimed to be a complete optimization procedure; rather it indicates the trend in the radiation of power as a function of the various factors and provides a value for the power that can be produced for comparison with other methods of acoustic transduction. To compare pressure levels, the USRD J9 projector is rated at a level of 150 dB re 1  $\mu$ Pa, at 1 kHz, which compares with a total emitted power of 0.01 W. The best case of Table B2, which appears to be realizable, has an output of 0.023 W.

#### APPLICATION TO TOROIDAL TRANSDUCER

The piston-type transducer described in the foregoing sections does not make essential use of the fluid properties of the material. In this section a configuration is proposed that does depend in a direct fashion on the fluid properties. The proposed configuration is vaguely reminiscent of the cylindrical geometry studied by Pclunin [15], which operates, though, in a magnetostrictive mode in the ultrasound region.

The ferrofluid is contained inside a toroidal space, which is bounded by a solid bottom and top and by cylindrical inner and outer walls made of an elastomer (Fig. 6). Both the dc bias field and the ac

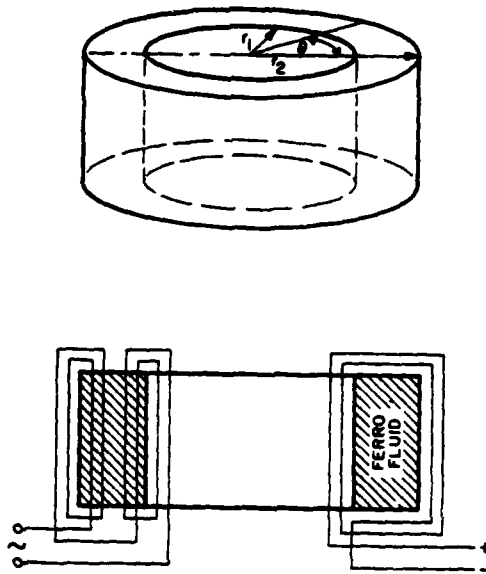


Fig. 6 — Perspective and cross section of toroidal transducer showing principle of dc and ac windings

excitation field are in the azimuthal direction and depend only on the radial distance; thus one has a magnetic field  $H_{\theta}(r)$ . The fields are created by current wires running in the axial direction. The force per unit volume and the ensuing velocity will be in the radial direction  $v_r(r)$ . Obviously, the current carriers should be rigid enough to withstand the mutually attractive forces. The stiffness can be improved by spacers in planes perpendicular to the axis which will not inhibit the flow other than by increased friction.

The windings providing the dc bias field can be applied in the usual toroidal manner. The ac-carrying wires can be arranged in different ways, but it would appear to be most advantageous to have part of their total number return through the inside of the toroid and the others at the outside. In this way, the ac magnetic field will straddle the dc field such that operation stays in the linear range. Cooling could be performed in the usual way by use of hollow conductors or by

separate cooling pipes, or it could be done by circulating the ferrofluid itself. The high viscosity (15 centipoise for H01-B fluid) would give some problems, though.

The equation of motion for this configuration would be

$$\rho_f \frac{\partial v_r}{\partial t} + \frac{\partial p}{\partial r} = \mu_o M_o \frac{\partial H_\theta}{\partial r} \quad (17)$$

and continuity

$$\frac{\partial (rv_r)}{\partial r} = 0 . \quad (18)$$

Thus the velocity depends on the radial distance by

$$v_r = v_o (r_2/r) , \quad (19)$$

where  $v_o$  is the radial velocity at the outer wall and the pressure at the outer wall is given by

$$\mu_o M_o \{H(r_2) - H(r_1)\} = p(r_2) + \frac{\partial v}{\partial t} r_2 \ln(r_2/r_1) \quad (20)$$

where H is calculated from the total current linked by the given circular path. Thus

$$H(r_2) - H(r_1) = (r_2 - r_1)J \quad (21)$$

for the case where  $H(r_1) = -H(r_2)$ .

The average current density J and the pressure at the inner wall are assumed constant.

The radiation resistance for a cylindrical radiator and its accession to inertia are given on pp 207-212 of Junger and Feit [14].

Infinite cylinders display a peculiar singular behavior near zero radius that is not expected for finite cylinders.

Detailed calculations have not been carried out, but it is expected that the power transfer is not essentially different from the piston design.

The major advantage of this configuration appears to be in the fact that here the dc and ac magnetic fields are brought close to and even inside the ferrofluid, so that in principle large transducers could be built for low frequencies. In the case of the piston, the fields are created outside the active medium and efficiency of solenoids goes down drastically when the bore diameter is increased.

#### CONCLUSIONS AND RECOMMENDATIONS

It appears that a piston type ferrofluid transducer (projector) can be constructed that is comparable in output power at a given physical size with that of a moving-coil projector (USRD Type J9). The piston concept does not make full use of the fluid properties of the material. A toroidal shape is proposed that would do so. Further analysis is necessary to show the technological feasibility of the latter configuration.

Contrary to the conclusion of Cary and Fenlon [6] it appears that ferrofluids have merit at lower frequencies as well. As a consequence, it may be worthwhile to reevaluate their other conclusion, namely, that ferrofluids are hardly to be considered a competitor for conventional magnetostrictive materials.

## REFERENCES

- [1] B. Berkovsky, editor, *Thermomechanics of Magnetic Fluids* (Hemisphere Publishing Corporation, Washington, 1978).
- [2] V. G. Bashtovoi and B. M. Berkovskii, "Thermomechanics of Ferromagnetic Fluids," *Magnitnaya Gidrodinamica*, 3, 3-14 (1973).
- [3] B. Berkovsky and R. E. Rosensweig, "Magnetic Fluid Mechanics: A Report on an International Advanced Course and Workshop," *J. Fluid Mech.* 87, 521-531 (1978).
- [4] A. R. V. Bertrand, "Les Ferrofluides," *Revue de l'Institut Français du Pétrole* 25, 16-34 (1970).
- [5] M. I. Shliomis, "Magnetic Fluids," *Soviet Physics Uspekhi*. 17, 153-169 (1974).
- [6] B. B. Cary and F. H. Fenlon, "On the Utilization of Ferrofluids for Transducer Applications," *J. Acoust. Soc. Am.* 45, 1210-1216 (1969).
- [7] J. W. Overby, "A Study of the Feasibility of Development of a Ferrofluid Transducer," Thesis, Florida Institute of Technology, 1978 (unpublished).
- [8] P. Penfield and H.A. Haus, *Electrodynamics of Moving Media* (M.I.T. Press, Cambridge, 1967).
- [9] T. B. Jones, "Theory and Application of Ferrofluid Seals" in *THERMOMECHANICS OF MAGNETIC FLUIDS*, edited by B. Berkovsky, (Hemisphere Publishing Co., Washington, 1978), pp 255-298.
- [10] B. M. Berkovsky, V. E. Fertman, V. K. Polevikov, and S. V. Isaev, "Heat Transfer Across Vertical Ferrofluid Layers," *International Journal of Heat and Mass Transfer* 19, 981-986 (1976).
- [11] C. P. Bean and J. D. Livingston, "Superparamagnetism," *J. Appl. Phys.* 30, 120S-129S (1930).
- [12] R. Kaiser and G. Miskolczy, "Magnetic Properties of Stable Dispersions of Subdomain Magnetite Particles," *J. Appl. Phys.* 41, 1064-1072 (1970).

- [13] E. H. Bogardus, R. Scranton, and D. A. Thompson, "Pulse Magnetization Measurements in Ferrofluids," *IEEE Transactions on Magnetics Mag* 11, 1364-1366 (1975).
- [14] M. C. Junger and D. Feit, *Sound, Structures, and Their Interaction* (M.I.T. Press, Cambridge, 1972).
- [15] V. M. Polunin, "A Method for the Resonance Excitation of Ultrasound in a Ferromagnetic Fluid," *Soviet Phys. Acoust.* 24, 52-54 (1978).
- [16] G. V. Brown, L. Flax, E. C. Itean, and J. C. Laurence, "Axial and Radial Magnetic Fields of Thick, Finite-Length Solenoids," NASA, TR R 170 (1963).

Appendix A  
PROPERTIES OF COMMERCIAL FERROFLUIDS

The following material is reproduced from "Ferrofluid Products" issued by the Ferrofluidics Corporation, 144 Middlesex Turnpike, Burlington, MA 01803.

Standard Ferrofluid Products

The carrier solvents used for standard fluids are designated aqueous, hydrocarbon, fluorocarbon, or diester. This selection of carriers gives a wide range of material properties for a variety of applications and test purposes.

A05: Aqueous Base - The aqueous or waterbase fluid is stabilized by an anionic surface active agent and is stable over a wide range of pH values. The particles are larger than the particles in other fluids by 15% and as a result exhibit a tendency to aggregate and chain in a magnetic field. The 200-gauss material is useful for Bitter magnetic-domain detection studies

H01: Hydrocarbon Base - The hydrocarbon fluid offers excellent stability and relatively low viscosity. The carrier is a refined white mineral oil. Although volatile it may be used in closed systems at temperatures in excess of 100°C for prolonged periods of time. The nominal electric resistivity is  $10^8 \Omega\text{cm}$  at 60 Hz, and the dielectric constant is 20 at 1 kHz. This is an excellent ferrofluid for research and development projects or to evaluate ferrohydrodynamic principles.

F08: Fluorocarbon Base - The fluorocarbon ferrofluid is based on a perfluoroalkylpolyether. This base material is the polymerization product of hexafluoropropyleneoxide. The ferrofluid has excellent chemical inertness, low vapor pressure and is completely nonflammable. It is immiscible

with most organic liquids except highly fluorinated solvents. The standard fluid is provided with viscosity of 500 centipoise at 27°C.

D01: Diester Base - This ferrofluid combines many useful properties, which make it the most widely used of ferrofluids. It has a low vapor pressure so that it can be used up to 110°C in open environments and at lower temperature in high-vacuum applications. It has excellent chemical stability to 120°C. The carrier is bis- (2 ethylhexyl) azelate which has the best viscosity-temperature performance of most organic fluids. The ferrofluid has excellent lubrication properties and has applications as a damping fluid. The standard fluid is available in viscosities of 100, 500, and 1000 centipoise at 27°C, giving an adequate range for most damping applications.

Table A1 - Typical Properties of Ferrofluids (25°C unless noted)<sup>a</sup>

MATERIAL	HYDROCARBON BASED		WATER BASED		DIESTER BASED	
	200	400	200	100	100	100
Magnetic Saturation, Gauss	1.05	1.25	1.18	1.19	1.19	1.19
Density, g/ml	3-10	5-25	1-10	100	500	1000
Viscosity, Centipoise (27°C)	4	7	0	-40	-35	-29
Pour Point (100,000 cp), °C	77	77		138	138	138
Vapor Pressure, temperature for 1 mm Hg, °C			100	324	324	324
760 mm Hg, °C	0.4	0.8	0.6	0.25	0.25	0.25
Initial Susceptibility, M/H	28	28	26	32	32	32
Surface Tension, dyne/cm	146	146	586	-	-	-
Thermal Conductivity, W/°C-cm <sup>3</sup> 10 <sup>5</sup>	0.43	0.55	1.0	-	-	-
Specific Heat, cal/°C-g	9.0	8.6	5.2	-	-	-
Thermal Expansion Coefficient, cm <sup>3</sup> /cm <sup>3</sup> °C <sup>3</sup> 10 <sup>4</sup> *						

<sup>a</sup> "Ferrofluid Products," Ferrofluidics Corp., Burlington, MA, Sep 1977

\* Average over range from 25 - 90°C

Appendix B  
SAMPLE CALCULATIONS OF ACOUSTIC POWER

The total power emitted by the piston and cone is the product of the following factors

$$\begin{array}{l}
 \text{I.} \quad \frac{1}{2} F_m^2 / (\rho c \pi R_1^2) \\
 \text{II.} \quad (R_1/a)^2 \\
 \text{III.} \quad (R_p / \rho c \pi a^2)^{-1} \\
 \text{IV.} \quad \frac{\left\{ \frac{R_p}{(\rho c) (\pi a^2)} \right\}^2}{\left\{ R_p / (\rho c \pi a^2) \right\}^2 + \left[ \left( \frac{\rho_f}{\rho} \right) \left( \frac{R_1}{a} \right)^2 \left( \frac{L}{a} \right) + \frac{M_p}{\pi \rho a^3} \right]^2} (ka)^2
 \end{array}$$

The sample calculations (Table B2) are intended to show the influence of the various factors on the total power. The radius  $R_1$  of the ferrofluid cylinder is not varied. The length  $L$  of the cylinder, radius  $a$  of the cone, and frequency are varied.

FACTOR I - This factor is not varied throughout the calculations. It represents power radiated at resonance, if the radiation resistance were that of a plane wave. The expression for  $F_m$  is given by

$$F_m = \mu_0 M_0 \overline{\Delta H_z} \pi R_1^2, \quad (\text{B1})$$

where

$$\overline{\Delta H_z} \pi R_1^2 = \int_0^{R_1} \Delta H_z 2\pi r dr.$$

Extensive tables for  $H_z$  in the field of a finite thick solenoid are given by Brown et al [16]. Since

$$H_z = \frac{1}{\mu r} \frac{\partial(rA_\phi)}{\partial r}. \quad (\text{B2})$$

where  $A\phi(r, z, \phi)$  is the azimuthal component of the vector potential, one sees that

$$(\pi R_1^2) \overline{H_z(z)} = (2\pi/\mu) R_1 A_\phi(R_1, z) \quad (B3)$$

and thus

$$\begin{aligned} \overline{(\Delta H_z)} (\pi R_1^2) &= (R_1) \int_{D/2}^{D/2+S} d\ell \int_{R_1}^{R_2} r J(r) dr \\ &\int_0^{2\pi} \cos\theta \left[ \left\{ \left( \frac{L}{2} \right) - \ell \right\}^2 + R_1^2 + r^2 - 2rR_1 \cos\theta \right]^{-\frac{1}{2}} \\ &- \left[ \left\{ \left( \frac{L}{2} \right) + \ell \right\}^2 + R_1^2 + r^2 - 2rR_1 \cos\theta \right]^{-\frac{1}{2}} d\theta . \quad (B4) \end{aligned}$$

where  $J(r)$  is the current density as a function of radial distance (see Fig. B1 for definition of configuration parameters). One might

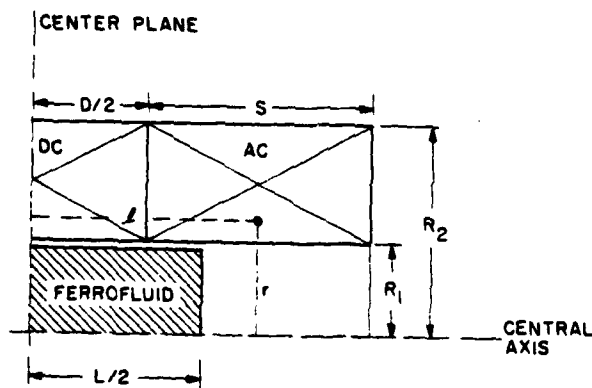


Fig. B1 - Definition sketch of solenoid arrangement

calculate this function directly. On the other hand, the variation of  $H(z)$  with  $r$  is not so drastic as to warrant this effort at the present time, where the tables of Brown give sufficiently extensive information for a first approach to the configuration of the coils needed.

To ensure approximate linear operation, one should choose the location of the operation point and the ac amplitude properly. From the  $M(H)$  curves, it appears that a value for  $H_0$  of 4000 Oe ( $3.2 \times 10^5$  A/m) and an amplitude of the modulation of 2000 Oe ( $1.6 \times 10^5$  A/m) would satisfy the requirement of approximate linearity. Thus  $\Delta H = 3.2 \times 10^5$  A/m. The saturation magnetization is 850 gauss ( $6.8 \times 10^4$  A/m) for the fluid used by J. Overby [7], which was especially manufactured for acoustic application. Its density  $\rho_f = 1.75$  g/cm<sup>3</sup>. The corresponding force  $F_m$  from Eq. (B1) is then found to be 34 N, and the first factor I is found to be 0.31 W.

FACTORS III and IV - The dimensionless expressions for radiation resistance  $R_p$  and accession to inertia  $M_p$  are given in Fig. B2 and Table B1. For small values of  $ka$ , one has the approximations

$$\frac{R_p}{\rho c \pi a^2} \approx \frac{1}{2} (ka)^2 \quad (B5)$$

and

$$\frac{M_p}{\rho \pi a^3} \approx \frac{8}{3\pi} \quad (B6)$$

and the average power is

$$\Pi = \left[ \frac{\frac{1}{2} F_m^2}{\rho c \pi R_1^2} \right] \left[ \frac{R_1}{a} \right]^2 \left[ \frac{1}{2} \left\{ \left( \frac{\rho_f}{\rho_m} \right) \left( \frac{R_1}{a} \right)^2 \left( \frac{L}{A} \right) + \frac{8}{3\pi} \right\}^{-2} \right] \quad (B7)$$

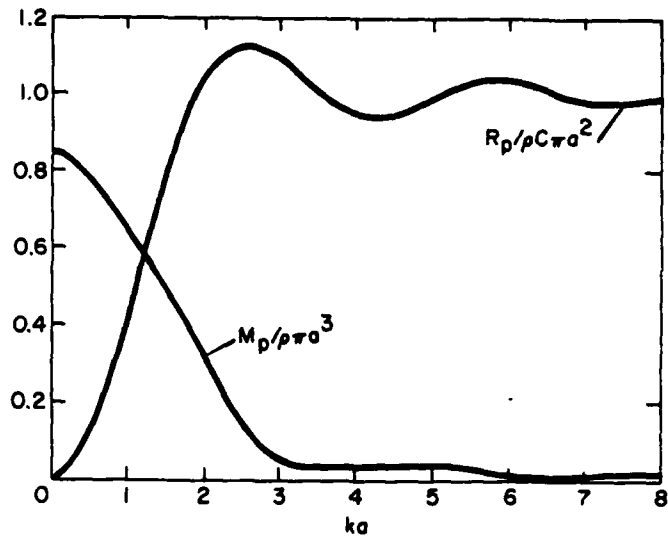


Fig. B2 - Radiation resistance and accessions to inertia

Table B1 - Impedance Functions for Circular Piston

ka	$R_p/\rho c \pi a^2$	$M_p/\rho \pi a^3$	ka	$R_p/\rho c \pi a^2$	$M_p/\rho \pi a^3$
0.0	0.0	0.8488	4.0	0.9413	0.0305
0.2	0.0198	0.8400	4.25	0.9357	0.0343
0.4	0.0779	0.8133	4.50	0.9455	0.0369
0.6	0.1695	0.7707	4.75	0.9661	0.0375
0.8	0.2876	0.7141			
1.0	0.4233	0.6468	5.0	0.9913	0.0357
1.2	0.5665	0.5718	5.25	1.0150	0.0318
1.4	0.7073	0.4931	5.50	1.0321	0.0221
1.6	0.8376	0.4139	5.75	1.0397	0.0211
1.8	0.9470	0.3378			
2.0	1.0330	0.2674	6.0	1.0372	0.0162
2.25	1.1027	0.1908	6.25	1.0265	0.0125
2.50	1.1310	0.1717	6.50	1.0108	0.0102
2.75	1.1242	0.0836	6.75	0.9944	0.0093
3.0	1.0922	0.0531	7.0	0.9809	0.0097
3.25	1.0473	0.0357	7.25	0.9733	0.0106
3.50	1.0013	0.0283	7.50	0.9727	0.0117
3.75	0.9639	0.0276	7.75	0.9784	0.0126
			8.0	0.9887	0.0128

It is significant that at small values of  $ka$  (low frequency), the emitted power is independent of frequency (ignoring resonance).

For large values of  $ka$  the approximations are

$$\frac{R_p}{\rho c \pi a^2} \approx 1. \quad (B8)$$

and

$$\frac{M_p}{\rho \pi a^3} = \frac{2}{\pi (ka)^2}. \quad (B9)$$

and the average power

$$\Pi = \left[ \frac{1}{2} \frac{F_m^2}{\rho c \pi R_1^2} \right] \left[ \frac{R_1}{a} \right]^2 \left[ \left( \frac{\rho_f}{\rho} \right) \left( \frac{R_1}{a} \right)^2 \left( \frac{L}{a} \right) \right]^{-2} \frac{1}{(ka)^2}. \quad (B10)$$

which decreases inversely proportional to the square of the frequency.

Table B2 - Sample Power Output Calculations

$R_1 = 2 \text{ cm}; \rho_f/\rho = 1.75$ Factor I = 0.31 watt	II	f Hz	ka	$R_p/\rho c \pi a^2$	$M_p/\rho \pi a^3$	III	IV	$\Pi$ watt
a = 4 cm; $R_1/a = 1/2$ L = 12 cm; L/a = 3	0.25	1000 500 100	$1.68 \times 10^{-1}$ $8.41 \times 10^{-2}$ $1.68 \times 10^{-2}$	$1.41 \times 10^{-2}$ $3.53 \times 10^{-3}$ $1.41 \times 10^{-4}$	0.85 0.85 0.85	$7.1 \times 10^2$ $2.81 \times 10^3$ $7.1 \times 10^1$	$1.00 \times 10^{-3}$ $3.78 \times 10^{-4}$ $1.51 \times 10^{-5}$	$8.1 \times 10^{-3}$ $8.3 \times 10^{-3}$ $8.3 \times 10^{-3}$
a = 4 cm; $R_1/a = 1/2$ L = 8 cm; L/a = 2	0.25	3000 1000 100	$5.04 \times 10^{-1}$ $1.68 \times 10^{-2}$ $1.68 \times 10^{-2}$	$1.20 \times 10^{-1}$ $1.41 \times 10^{-2}$ $1.41 \times 10^{-4}$	0.80 0.85 0.85	8.3 $7.1 \times 10^2$ $7.1 \times 10^1$	$1.98 \times 10^{-2}$ $2.36 \times 10^{-3}$ $2.37 \times 10^{-5}$	$1.27 \times 10^{-2}$ $1.27 \times 10^{-2}$ $1.30 \times 10^{-1}$
a = 6 cm; $R_1/a = 1/3$ L = 18 cm; L/a = 3	0.11	1000	$2.51 \times 10^{-1}$	$3.12 \times 10^{-2}$	0.85	$3.2 \times 10^1$	$7.49 \times 10^{-3}$	$8.27 \times 10^{-3}$
a = 4 cm; $R_1/a = 1/2$ L = 4 cm; L/a = 1	0.25	1000 100	$1.68 \times 10^{-1}$ $1.68 \times 10^{-1}$	$1.41 \times 10^{-2}$ $1.41 \times 10^{-4}$	0.85 0.85	$7.1 \times 10^3$ $7.1 \times 10^1$	$4.23 \times 10^{-3}$ $4.25 \times 10^{-5}$	$2.33 \times 10^{-2}$ $2.33 \times 10^{-2}$
a = 2 cm; $R_1/a = 1$ L = 4 cm; L/a = 2	1.00	100	$8.4 \times 10^{-3}$	$3.61 \times 10^{-5}$	0.85	$2.8 \times 10^4$	$9.7 \times 10^{-7}$	$8.3 \times 10^{-3}$